

Article ID: 1007-4627(2013)03-0278-06

# Tetrahedral Symmetry in Superheavy Nuclei

CHEN Yongshou, GAO Zaochun

(China Institute of Atomic Energy, Beijing 102413, China)

**Abstract:** The projected energy surface calculations based on the reflection asymmetric shell model predict that nucleus  $^{310}126$  is the doubly magic nucleus next to  $^{208}\text{Pb}$  and has a tetrahedral shape in its ground state. The tetrahedral symmetry-driven quantal effects may lead to an increase of binding energy of the ground state by about 13 MeV with respect to the corresponding spherical shape, indicating the importance of inclusion of the tetrahedral degree of freedom in calculations for the heaviest nuclei. The results show that the tetrahedral symmetry-driven quantal effects can significantly increase the fission barriers and therefore result in increased survival probabilities of superheavy nuclei.

**Key words:** shell model; tetrahedral symmetry; superheavy nuclei

**CLC number:** O572.21; O571.6    **Document code:** A    **DOI:** 10.11804/NuclPhysRev.30.03.278

## 1 Introduction

The tetrahedral symmetry that breaks spontaneously both the spherical symmetry and the symmetry by inversion has been identified in molecules, fullerenes, metal clusters and many other quantum objects, all of which are governed by electromagnetic interaction. The possibility that atomic nuclei, as a strong interaction finite many-body quantum system, have their low-lying states of tetrahedral symmetry is definitely interesting for all related domains of physics. Recently, a number of publications have focused on the possibility of an unambiguous discovery of the tetrahedral symmetric nuclei. The low-lying tetrahedral states was predicted by the potential energy surface calculations to appear in  $^{156}\text{Gd}$  and then the candidate tetrahedral band was suggested to be the previously measured lowest negative-parity band with the spin-parity sequence of  $1^-, 3^-, 5^-, \dots$ <sup>[1]</sup>. Due to the rule governed by the tetrahedral symmetry the tetrahedral band should have very small reduced electric quadrupole transition probabilities,  $B(E2)$ , between its band states of  $\Delta I = 2$ . Recently, to test the tetrahedral symmetry the ultrahigh-resolution  $\gamma$ -ray spectroscopy of  $^{156}\text{Gd}$  was carried out in a collaboration between France, Poland, Bulgaria, Switzerland and

Italy<sup>[2]</sup>. They first identified the  $5_1^- \rightarrow 3_1^-$  transition of 131.983 keV and then measured the lifetime of the  $5_1^-$  state using the GRID technique. The resulting  $B(E2)$  leads to the intrinsic quadrupole moment of the  $5_1^-$  state in  $^{156}\text{Gd}$  to be 7.1 b, which is comparable to the quadrupole moment of the ground state in the nucleus. This experimental result gives strong evidence against tetrahedral symmetry in the lowest negative-parity band of  $^{156}\text{Gd}$ . The same conclusion for the non-tetrahedral symmetry of this negative-parity band also was drawn by another experimental data<sup>[3]</sup>. The present work will focus on the possibility of the new candidate of tetrahedral symmetry in the superheavy region.

Another fundamental question has long been prediction and/or production of the heaviest doubly magic nucleus next to  $^{208}\text{Pb}$ . Among the modern theoretical studies, the predicted proton magic numbers are quite scattered while the neutron magic numbers are relatively common to be  $N = 184$ . For example, within the Skyrme-Hartree-Fock approach and the relativistic mean-field model the doubly magic superheavy nuclei are predicted to be  $^{298}114$ ,  $^{292}120$ ,  $^{308}124$ , and  $^{310}126$ , depending on the parameterization<sup>[4-5]</sup>. The nuclei with  $Z \geq 120$  were predicted to be spherical and to have vanishingly low fission

**Received date:** 29 Oct. 2012;    **Revised date:** 15 Mar. 2013

**Foundation item:** National Natural Science Foundation of China (11175258, 11021504, 11275068)

**Biography:** CHEN Yongshou(1939-), male, Luzhou, Sichuan, China, Professor, working on the field of theoretical nuclear physics, nuclear astrophysics; E-mail: yschen@ciae.ac.cn

<http://www.npr.ac.cn>

barriers, indicating a little chance to extend the chart into the island of superheavy elements. In the present work, we consider the tetrahedral symmetry which may result in considerably larger shell effects than the spherical symmetry, so that the proposed doubly magic superheavy nuclei could significantly gain the binding effects in their tetrahedral states.

The tetrahedral symmetry corresponds to the invariance under the transformation of the double point group  $T_d^D$  whose irreducible representations can lead to fourfold (in addition to twofold) degeneracies of single-particle spectra<sup>[6]</sup>. This aspect of high degeneracy leads to the high stability of nuclear systems. Information related to the tetrahedral symmetry in the superheavy region has been only seen in the  $\gamma$ -ray spectroscopy of transfermium nuclei. The low-lying negative parity bands with  $I^\pi = 2^-, 3^-, 4^-, 5^-, \dots$  have been observed in the isotones of  $N = 150$ ,  $^{246}\text{Cm}$ ,  $^{248}\text{Cf}$ ,  $^{250}\text{Fm}$  and  $^{252}\text{No}$ . The transfermium nuclei are the gateway of the superheavy region and only heaviest nuclei yet studied with spectroscopy. The occurrence of the tetrahedral degree of freedom in the transfermium nuclei implies that the tetrahedral symmetry could be an important factor that influences the structure of superheavy elements. In the present work, we carry out the projected energy surface (PES) calculation based on the reflection asymmetric shell model (RASM) to investigate the tetrahedral symmetry in superheavy nuclei.

For description of nuclear shape, it has been proven to be very useful to parameterize the surface  $R(\theta, \phi)$  through its expansion in the spherical harmonic function  $Y_{\lambda\mu}^*(\theta, \phi)$ , where  $\theta$  and  $\phi$  are the rotation angles<sup>[7]</sup>. The coefficients of the expansion stand for deformation parameters. The quadrupole deformation ( $\lambda = 2$ ) is the leading deformation effect known for almost all the isotopes throughout the chart of nuclides. The axial octupole  $Y_{30}$  deformation, related to the spontaneous breaking of reflection symmetry, is known in the several mass regions<sup>[8]</sup>. The tetrahedral symmetry is realized at the first order through the nonaxial octupole  $Y_{32}$  deformation<sup>[9]</sup>, which describes a tetrahedral, ‘pyramid-like’, shape.

A brief description of the model is given in Section 2. The results of calculations and their implications in the structure and the stability of superheavy nuclei are presented in Section 3. A summary is in Section 4.

## 2 Brief description of theory

The energy surface calculation is a powerful means to study deformed nuclei. The PES calculation based on the RASM applies to the study of deformed nuclear states with good angular momentum and parity. The wave function of the RASM is written in terms of projected multi-quasiparticle (qp) states, for the details of the model see Refs. [10–11]

$$|\Psi_{I^{\pi}M}\rangle = \sum_{K\kappa} f_{K\kappa}^{I^{\pi}} \hat{P}^{\pi} \hat{P}_{MK}^I |\phi_{\kappa}\rangle. \quad (1)$$

Here the index  $\kappa$  labels deformed basis states, and  $\hat{P}^{\pi}$  and  $\hat{P}_{MK}^I$  are the parity-projection and angular-momentum-projection operators, respectively. For even-even nuclei,  $|\phi_{\kappa}\rangle$  stands for  $\{|0\rangle, a_{\nu}^{\dagger} a_{\nu}^{\dagger} |0\rangle, a_{\pi}^{\dagger} a_{\pi}^{\dagger} |0\rangle, \dots\}$ , where  $a_{\nu}^{\dagger}$  and  $a_{\pi}^{\dagger}$  are the qp creation operator for neutrons and protons, respectively, with respect to the qp vacuum  $|0\rangle$ . The qp states are obtained from a deformed Nilsson calculation followed by BCS calculation, in a model space with four major shells ( $N = 5 \sim 8$  for neutrons and  $N = 4 \sim 7$  for protons). The deformed Nilsson calculation is performed with the quadrupole and octupole terms, which break the rotation and reflection symmetries, respectively. The broken symmetries are necessarily restored in the laboratory frame by the projections.

Using the trial wave function of Eq. (1) we obtain the variational equation for the Hamiltonian  $H$ ,

$$\delta \langle \Psi | H | \Psi \rangle - E \delta \langle \Psi | \Psi \rangle = 0. \quad (2)$$

By carrying out the variational procedure with respect to the wave function, precisely the coefficients  $f_{K\kappa}^{I^{\pi}}$ , we obtain the eigenvalue equation,

$$\sum_{K\kappa} f_{K\kappa}^{I^{\pi}} (\langle \Phi_{\kappa} | H P^{\pi} P_{K'K}^I | \Phi_{\kappa} \rangle - E \langle \Phi_{\kappa} | P^{\pi} P_{K'K}^I | \Phi_{\kappa} \rangle) = 0, \quad (3)$$

and the normalization condition,

$$\sum_{K\kappa'K\kappa} f_{K'\kappa'}^{I^{\pi}*} \langle \Phi_{\kappa'} | P^{\pi} P_{K'K}^I | \Phi_{\kappa} \rangle f_{K\kappa}^{I^{\pi}} = 1. \quad (4)$$

By solving the eigenvalue equation one obtains the wave functions and the energies of band states. These eigenenergies have good angular momentum and good parity and, therefore, can directly compared with the experimental data.

By using the RASM wave function, the angular-momentum- and parity- projected energy

$$E^{Ip} = \frac{\langle \Psi_{Ip} | \hat{H} | \Psi_{Ip} \rangle}{\langle \Psi_{Ip} | \Psi_{Ip} \rangle} \quad (5)$$

is calculated in the space of quadrupole and tetrahedral deformations ( $\epsilon_2$ ,  $\epsilon_{32}$ ). The quadrupole deformation is most important competing effect to distort the tetrahedral symmetry. Within this two-dimension space the observed tetrahedral structures in transfermium nuclei have been well described. In principle, the energies calculated with  $\Psi_{Ip}$  of Eq. (1) have advantages over those with unprojected states  $|\phi_\kappa\rangle$ . The projection treats the states full quantum-mechanically by collecting all the energy-degenerate mean field states. The projections create a superposition of states in the Euler space and the reflection space, lowering the total energy of the system.

The Hamiltonian has the form

$$\hat{H} = \hat{H}_0 - \frac{1}{2} \sum_{\lambda=2}^3 \chi_\lambda \sum_{\mu=-\lambda}^{\lambda} \hat{Q}_{\lambda\mu}^\dagger \hat{Q}_{\lambda\mu} - G_0 \hat{P}_{00}^\dagger \hat{P}_{00} - G_2 \sum_{\mu=-2}^2 \hat{P}_{2\mu}^\dagger \hat{P}_{2\mu}. \quad (6)$$

Here  $\hat{H}_0$  is the spherical single particle Hamiltonian, the second term contains the quadrupole-quadrupole (Q-Q) and octupole-octupole (O-O) interactions, and the third and last terms are the monopole and quadrupole pairing forces, respectively. The interaction strengths  $\chi_\lambda$  are usually determined with given deformations through the self-consistent relations<sup>[11]</sup>. In the PES calculation, there is an ambiguity in determining the strengths. By considering the smooth variation of the strength in the deformation plane, we calculate the common strengths using the middle points in the deformation ranges, the way is similar to Ref. [12]. The  $\chi_\lambda$ -values are listed in Table 1.

**Table 1** The interaction strengths  $\chi^{\tau\tau'}$  (in MeV) for Q-Q and O-O forces, where  $\tau$  denotes protons or neutrons

	$\chi^{nn}$	$\chi^{pp}$	$\chi^{np} = \chi^{pn}$
Q-Q	0.0208	0.0162	0.0184
O-O	0.0152	0.0118	0.0134

The monopole pairing strength has a standard form  $G_0 = \frac{G}{A}$ , where  $A$  is the mass number. In the present calcula-

tions,  $G = 15.5$  MeV is taken for both protons and neutrons, which leads to a reasonable odd-even mass difference in the mass region. The quadrupole pairing strength is  $G_2 = 0.12G_0$  as usual. The deformed single-particle states are calculated using the Nilsson potential with the standard parameters<sup>[13]</sup>, and including the nonaxial-octupole term of  $\epsilon_{32} \sqrt{\frac{\pi}{7}} r^2 (Y_{32} + Y_{3-2})$  in the Hamiltonian.

### 3 Results and discussion

The RASM calculations have well reproduced the observed low-lying states in the transfermium nuclei<sup>[11]</sup>. As an example, the solution of the eigenvalue equation, Eq. (3), for  $^{252}\text{No}$  is carried out. Fig. 1 shows a comparison between the experimental data and the low-lying rotational bands calculated with deformation parameters of  $\epsilon_2 = 0.235$  and  $\epsilon_{32} = 0.107$  for this nucleus. It is seen that the experimental lowest positive- and negative-parity bands are well reproduced by the RASM calculation. The parity splitting, which measures how higher in energy the negative-parity band lies above the positive-parity ground band, sensitively depends on the tetrahedral deformation,  $\epsilon_{32}$ . The parity splitting and its quenching with increasing spin have been well reproduced with an adequate value of  $\epsilon_{32}$ , as shown in Fig. 1.

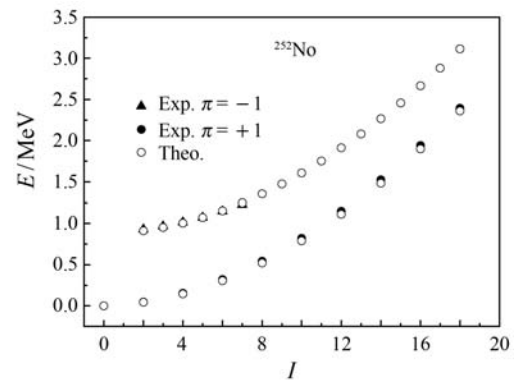


Fig. 1 Calculated low-lying negative- and positive-parity bands for  $^{252}\text{No}$  are compared with the experimental data taken from Ref. [14].

The  $Y_{32}$  couplings between the shell states with  $\Delta j = \Delta l = 3$  ( $j$  and  $l$  are the total and orbit angular momenta, respectively) lead to the rearrangement of s.p. levels so that the tetrahedral shell gaps are formed. According to this rule, it is expected that in the superheavy region the strong tetrahedral correlation (or deformation) may be generated by the  $Y_{32}$  couplings between the proton  $i_{13/2}$  and

$f_{7/2}$  shell states, between the proton  $i_{11/2}$  and  $f_{5/2}$  shell states, between the neutron  $j_{15/2}$  and  $g_{9/2}$  shell states and between the neutron  $h_{11/2}$  and  $d_{5/2}$  shell states. Indeed, the  $Y_{32}$  couplings between these shell states are responsible for the formation of tetrahedral shell gaps appearing in the s.p. diagram, the single-particle energies in function of tetrahedral deformation  $\epsilon_{32}$  while the quadrupole deformation kept at  $\epsilon_2 = 0$ . There are the proton shell gaps of  $Z = 100$  and  $Z = 124 \sim 126$  at around  $\epsilon_{32} = 0.15$  and  $0.3$ , respectively, and the neutron shell gaps of  $N = 154$  and  $N = 184$  at around  $\epsilon_{32} = 0.25$  and  $0.3$ , respectively. The nucleus may have tetrahedral shape when the Fermi level lies in the vicinity of a tetrahedral shell gap. The occurrences of the tetrahedral structures observed in the transfermium isotones with  $N = 150$  and  $Z = 96 \sim 102$  is related to the tetrahedral shell gaps of  $N = 154$  and  $Z = 100$ . Similarly, the tetrahedral shell gaps of  $Z = 126$  and  $N = 184$  indicate the possible occurrence of the tetrahedral structures in the heaviest nuclei.

The Strutinsky's shell correction energy,  $E_{\text{shell}}$ , is a useful quantity to measure the shell effect. This quantity is sensitive to the shell gap structure in the s.p. diagram and has a largest negative value when the Fermi-level lies at a shell gap. Fig. 2 shows the calculated  $E_{\text{shell}}$  for  $^{310}126$  nucleus in function of  $\epsilon_{32}$  for given values of quadrupole deformation  $\epsilon_2$ . The curve with  $\epsilon_2 = 0$  illustrates how the quantity varies from spherical to tetrahedral shapes with increasing  $\epsilon_{32}$ . The largest negative  $E_{\text{shell}}$  of about  $-8.5$  MeV presents at  $\epsilon_{32} = 0.3$  and  $\epsilon_2 = 0$ , implying that the shell effects favor a strongly deformed tetrahedral shape

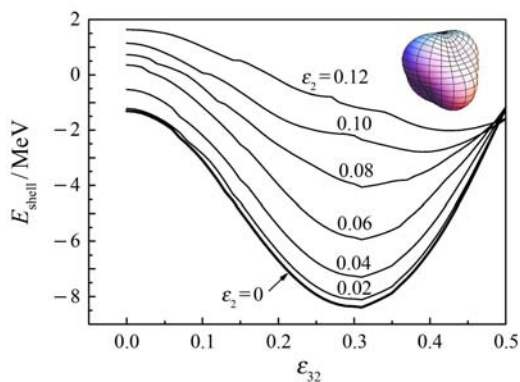


Fig. 2 (color online) Strutinsky's shell correction energy of  $^{310}126$  nucleus in function of tetrahedral deformation  $\epsilon_{32}$  for given quadrupole deformation  $\epsilon_2$ . The curves are labelled by their  $\epsilon_2$  values. The sketch at the upper-right corner illustrates a tetrahedral shape with  $\epsilon_{32}=0.3$ .

for the  $^{310}126$  nucleus. The shell energy difference between the tetrahedral and spherical shapes is about  $-7$  MeV, indicating the greater stabilizing effect of tetrahedral symmetry than the spherical symmetry. The curves with small quadrupole deformations also have the well defined minima of  $E_{\text{shell}}$  at around the same value of  $\epsilon_{32} = 0.3$ . This implies the stability of tetrahedral symmetry against the obscuration of the quadrupole deformation. The large shell correction energy induced by the tetrahedral symmetry provides the foundation for the establishment of the tetrahedral ground state in  $^{310}126$ . We will see that this conclusion is even strengthened by the present PES calculation below.

In the present study we investigate the tetrahedral symmetry in the ground state (g.s.) and low-energy states with spin  $I \leq 8$ . Therefore, only the BCS vacuum  $|0\rangle$  configuration needs to be included in the PES calculations, and the contributions from multi-qp configurations are negligible. Fig. 3 shows the calculated PES in  $^{310}126$  nucleus for the ground state of  $I^\pi = 0^+$ . The PES for the g.s. shows a well established minimum at  $\epsilon_2 = 0.02$  and  $\epsilon_{32} = 0.3$ . This result strongly supports the tetrahedral symmetry of nucleus  $^{310}126$  in its ground state, where the quadrupole deformation is vanishingly small and the tetrahedral deformation is large. The energy at the minimum is lowered by  $13.5$  MeV and  $7.9$  MeV compared to the spherical and saddle point, respectively, implying the large quantal effect of tetrahedral symmetry on the binding of the system. The

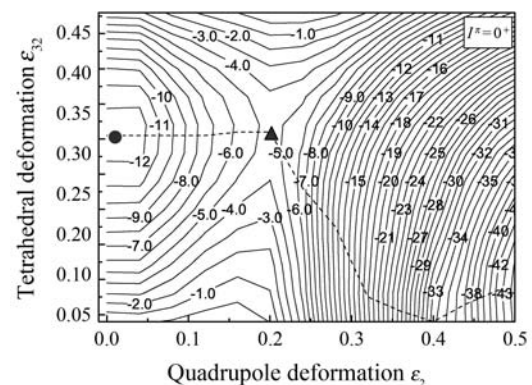


Fig. 3 Calculated PES of the  $^{310}126$  nucleus in function of the quadrupole ( $\epsilon_2$ ) and tetrahedral ( $\epsilon_{32}$ ) deformations for the ground state of  $I^\pi = 0^+$ .

The solid circle and triangle denote the minimum and saddle points, respectively. The dashed line denotes the fission trajectory. The contour scale is  $1.0$  MeV and the energy is normalized to be zero for the spherical shape.

result demonstrates that the inclusion of tetrahedral degree of freedom is very important in the calculations for the heaviest nuclei. The lowering of energy induced by tetrahedral deformation also presents in the shell correction energy, as shown in Fig. 2. However, the amount of lowered energy is much larger for the projected energy than for the shell correction one. The reason is that the dynamic octupole correlations and projections in the RASM, as the beyond-mean-field effects, are not incorporated in the Strutinsky's shell energy calculation. We note that despite the differences the PES and shell correction energy calculations result in almost the same tetrahedral shape for the  $^{310}126$  nucleus.

Similar to the g.s., the calculated PES.s for the low-lying states also have their local minima at  $\epsilon_{32} \approx 0.3$  and  $\epsilon_2 \approx 0.02$ . The strongly deformed tetrahedral minima found not only for the g.s. but also for many low-lying states demonstrate that the tetrahedral symmetry is well established in the  $^{310}126$  nucleus.

The PES calculation allows us to determine the fission barrier for the state with good angular momentum and parity. Fig. 4 shows the fission barrier for the ground state in the  $^{310}126$  nucleus. The increase of the fission barrier in both height and width implies an increase of the fission lifetime. In the calculation of fission barrier for the heaviest nuclei, the inclusion of tetrahedral deformation is important because the tetrahedral degree of freedom can strongly affect the shape of the fission barrier. As shown in Fig. 4, the calculated fission barrier without tetrahedral deformation is almost zero in height, while the tetrahedral

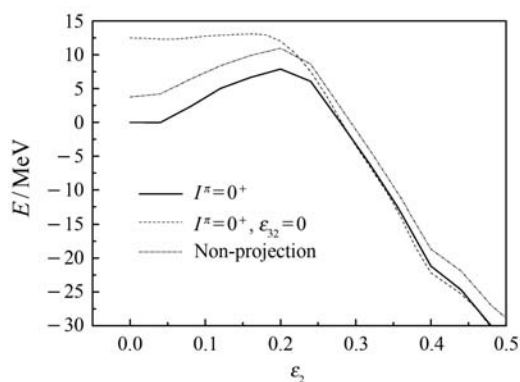


Fig. 4 Calculated fission barrier of the  $^{310}126$  nucleus for the q.s.(solid). The fission barrier calculated with  $\epsilon_{32} = 0$  (dash) and calculated without the projection (dash dot). The energy is normalized to be zero for the spherical shape.

calculation results in a fission barrier height of about 7.9 MeV and a much larger width. The calculation without projection results in a fission barrier height of 7.2 MeV, indicating that the projection leads to an increase of the barrier height by only few percent, although its effect on the energy lowering is large. We note that the fission barrier shown in Fig. 4 is not realistic as the nuclear fission barrier is determined by other complex dynamic processes which are not included in the present model. However, it is expected that the tetrahedral symmetry-driven quantal effects, which are fully described by the model, may strongly affect the real fission barrier.

The PES calculations also have been performed for the isotones of  $N = 184$  with  $Z = 120, 122$  and  $124$ . The results show that their ground and low-lying states are tetrahedrally shaped, similar to the  $^{310}126$  nucleus. For the ground states of the  $N = 184$  isotones with  $Z = 120, 122, 124$  and  $126$ , the equilibrium tetrahedral deformations are  $\epsilon_{32} = 0.24, 0.28, 0.28$  and  $0.30$  and the energy differences between the tetrahedral and spherical shapes are  $-5.9, -8.1, -11.1$  and  $-13.5$  MeV, respectively. With the largest energy lowering with respect to spherical shape, the tetrahedral nucleus  $^{310}126$  may be suggested as the doubly magic nucleus next to  $^{208}\text{Pb}$ .

The prediction of the tetrahedral doubly magic superheavy nucleus has been the subject of exceptional difficulty so that different conclusions could be drawn from the same types of calculations. For example, the recent total potential energy (TPE) calculation in Ref. [15] cannot confirm the existence of tetrahedral magic numbers predicted by another calculation in Ref. [16]. In these calculations, the macroscopic-microscopic model with Woods-Saxon potential is used. In Ref. [15], the calculations with a large deformation space (12 dimensions) result in so called conditional ( $\beta_2 = 0$ ) tetrahedral minima showing the occurrence of the tetrahedral symmetry for superheavy nuclei around  $Z = 124$  and  $N = 186$ , similar to the present PES calculations and the calculations of Ref. [16]. However, the global tetrahedral minima reported in Ref. [15] are different than Ref. [16] because of their different macroscopic (Liquid Drop) parameterizations. In fact, the difference energy of only about 0.5 MeV between the tetrahedral and spherical minima leads to the conclusion of the absence of the tetrahedral nucleus ( $Z = 124, N = 186$ ) in Ref. [15]. The present work investigates the nuclear tetrahedral stability

in terms of nucleonic degrees of freedom. It includes not only the shell effects but also the beyond mean field effects. As shown above, in addition to the shell correction energy, the extra lowered energy induced by the projections is large enough, about  $3 \sim 4$  MeV, to remove the bifurcation between Refs. [15-16]. Then, how to incorporate the beyond mean field effects into the more realistic models is our next task.

## 4 Summary

In summary, we have investigated the tetrahedral symmetry and doubly magic nucleus in the superheavy mass region using the PES calculations based on the RASM. The tetrahedral g.s. and low-lying states are predicted to be the occurrences in the superheavy elements. The doubly magic nucleus next to  $^{208}\text{Pb}$  has been predicted to be the  $^{310}126$  and well tetrahedrally shaped in its ground state. The strong tetrahedral symmetry-driven quantal effects increase the barrier to fission and therefore result in increased survival probabilities of superheavy nuclei. For the heaviest nuclei previously predicted to have an extremely short lifetime, we have discussed the possibility of inversion of stability, in that the tetrahedral states can be significantly longer-lived than the corresponding spherical states. The further studies of tetrahedral states will provide essen-

tial tests, not only of our specific predictions for the tetrahedral structures, but also of the new symmetry of the nuclear mean field.

## References:

- [1] DUDEK J, CURIEN D, DUBRAY N, *et al.* Phys Rev Lett, 2006, **97**: 072501.
- [2] JENTSCHHEL M. Phys Rev Lett, **104**, 222502(2010).
- [3] BARK R A. Phys Rev Lett, 2010, **104**: 022501.
- [4] BENDER M, RUTZ K, REINHARD P G, *et al.* Phys Rev C, 1999, **60**: 034304.
- [5] KRUPPA A T. Phys Rev C, 2000, **61**: 034313.
- [6] LI X, DUDEK J. Phys Rev C, 1994, **49**: R1250.
- [7] BOHR A, MOTTELSON R B. Nuclear Structure Vol II[M]. New York: Benjamin Inc, 1975.
- [8] BUTLER P, NAZAREWICZ W, Rev Mod Phys, 1996, **68**: 349.
- [9] ZBERECKI K, MAGIERSKI P, HEENEN P H, *et al.* Phys Rev C, 2006, **74**: 051302(R).
- [10] CHEN Y S, GAO Z C. Phys. Rev C, 2000, **63**: 014314.
- [11] CHEN Y S, SUN Y, GAO Z C. Phys Rev C, 2008, **77**: 061305(R).
- [12] ENAMI K I. Prog Theo Phys, 2000, **104**: 757.
- [13] BENGTTSSON T, RAGNARSSON I. Nucl Phys A, 1985, **436**: 14.
- [14] SULIGNANO B. EPJA, 2007, **33**: 327.
- [15] JACHIMOWICZ P. Int J Mod Phys E, 2011, **20**: 514.
- [16] MAZUREK K. Acta Physica Pol B, 2009, **40**: 731.

## 超重核的四面体对称性

陈永寿<sup>1)</sup>, 高早春

(中国原子能科学研究院, 北京 102413)

**摘要:** 基于反射不对称壳模型的投影位能面计算预言原子核  $^{310}126$  是继  $^{208}\text{Pb}$  之后的双幻核, 其基态呈现出四面体形状。四面体对称性驱动的量子效应可以使基态的结合能, 相较球形而言增加达 13 MeV, 这反映了在最重核的计算中, 考虑四面体自由度的重要性。计算结果还表明, 四面体对称性驱动的量子效应能够明显地增加裂变位垒, 从而导致超重核合成几率的增加。

**关键词:** 壳模型; 四面体对称性; 超重核

收稿日期: 2012-10-29; 修改日期: 2013-03-15

基金项目: 国家自然科学基金资助项目(11175258, 11021504, 11275068)

1) E-mail: yschen@ciae.ac.cn

<http://www.npr.ac.cn>